New developments for the use of microphysical variables for the assimilation of IASI radiances in convective scale models

P.Martinet[1], N.Fourrié[1], V.Guidard[1], F.Rabier[1], T.Montmerle[1], P.Brunel[2], L.Lavanant[2]

[1]*Météo France & CNRS/CNRM-GAME*

[2]*Météo France, Centre de Météorologie Spatiale*

Introduction

Nowadays, satellite observations are an important source of data assimilated in numerical weather prediction (NWP) models. They contribute positively to NWP analysis and the accuracy of forecasts (Kelly and Thépaut 2007).

The Infrared Atmospheric Sounding Interferometer (IASI) on-board the MetOp satellite belongs to a new generation of advanced infrared sounders and follows the launch of the Atmospheric InfraRed Sounder (AIRS) on-board the Aqua satellite in 2002. AIRS with 2378 channels and IASI with 8461 channels provide information about atmospheric temperature and humidity with a far better spectral resolution compared to previous instruments such as the High Resolution InfraRed Sounder (HIRS). All the NWP centres intend to increase the number of assimilated satellite observations which are limited, most of the time, to clear-sky locations. For instance, only 3% of the screened radiances are used in the operational data assimilation at the European Centre for Medium-Range Weather Forecast (ECMWF) according to Kelly and Thépaut (2007). This under-exploitation of satellite data is partly caused by a rejection of cloud-affected radiances during the assimilation process because of large innovations (observation minus background) due to cloud mislocation or deficiencies in the modelling of clouds, either in radiative transfer (RT) models or NWP models. The high correlation between cloud cover and meteorologically sensitive areas underlines the need to use infrared observations in presence of clouds (McNally 2002, Fourrié and Rabier 2004).

Nevertheless, an incorrect modelling of clouds leads to increased errors in the RT calculations especially in the infrared (IR) spectral range which is very sensitive to cloud microphysical properties. Different techniques have been developed in the frame of global models to overcome this problem. The first one was to reject all the observations classified as cloudy using sophisticated screening procedures (English et al 1999). This led to a poor yield in terms of exploited soundings. Instead of identifying clear-sky locations, McNally and Watts 2003 developed a method to detect clear channels from high-resolution IR spectra to assimilate channels unaffected by clouds even in a cloud-affected sounding.

Pavelin et al 2008 showed that it is possible to assimilate cloud-affected infrared radiances when retrieved cloud parameters are used as set constraints. The cloud-top pressure (CTOP) and the effective cloud fraction (Ne) are first retrieved by a one-dimensional variational data assimilation system (1D-Var) and then transferred to the four-dimensional variational data assimilation (4D-Var) for the assimilation of cloud-affected radiances. This method has shown to improve significantly the analysis profiles over the first guess and is used operationally at the Met Office to assimilate AIRS and IASI cloud-affected radiances. Recently, McNally 2009 has used the two cloud parameters (CTOP and Ne) to directly assimilate cloud-affected IR radiances. Two channels are used to determine the cloud parameters which are then introduced into the analysis control vector of the 4D-Var system of the global NWP model of the ECMWF. The cloud parameters are used only to constrain the minimisation but are not included in the model fields used for the forecasts.

In this study, we propose new developments for the assimilation of cloud-affected radiances taking advantage of the high resolution of convective scale NWP models. Their kilometre-size grid mesh, non-hydrostatic equations and microphysics parameterizations enable a better

modelling of cloud variables such as liquid water content (ql), ice water content (qi) and cloud fraction.
However, the assimilation of satellite data in mesoscale model creates new problems such as scale differences between model and satellite measurements. In fact, such NWP models are generally one order smaller than any satellite observation field of view.
The main purpose of this paper is to assess the feasibility of adding cloud profiles (ql,qi) in the control vector of a 1D-Var assimilation system preparing for the direct assimilation of such profiles in the three-dimensional variational data assimilation (3D-Var) system of the French operational AROME model (Seity et al 2011).
To prepare the 1D-Var, an observation-screening procedure permitting an improved selection of homogeneously covered scenes from IASI observations was developed. The feasibility of using cloudy fields from mesoscale NWP models to simulate cloudy radiances was investigated. To that end, the fast RT model RTTOV has been used to improve the simulation of multi layer clouds. We evaluated the simulated cloud-affected radiances and their departures from observations. Finally, some 1D-Var experiments, using cloud-affected IASI radiances are presented.

Experimental framework

In order to convert atmospheric profiles from the NWP model into simulated radiances, the fast radiative transfer model RTTOV is used. The version 10.1 of RTTOV (Hocking et al 2010) used in this study contains an advanced interface to include ql, qi and cloud fraction profiles called RTTOVCLD hereafter. The advanced interface RTTOVCLD enables a better modelling of clouds with the possibility of multi-layer clouds and two cloud types per layer. Absorption is computed in each of the 101 fixed vertical levels from the interpolated cloudy profiles using fast transmittance coefficients calculated by the line-by-line transmittance model LBLRTM.
The convective scale model AROME (Application of Research to Operations at MEsoscale) with a 2.5 km grid mesh is used to provide cloudy profiles over the Mediterranean Sea during a period of 30 days (7 October 2010 to 7 November 2010).

Selection of homogeneously covered scenes

The assimilation of cloudy radiances in convective scale models is an innovative challenge.
Focusing on homogeneously covered scenes avoids many complications associated with the forward modelling and analysis of fractional clouds.
The agreement between observations and simulations from the background is also improved with this selection. This condition is necessary to respect the linearity in the vicinity of the background required by variational assimilation methods
The selection of cases seen as homogeneous by both IASI and AROME also avoids deficiencies in the analysis and non-Gaussian distribution for background errors caused by a mislocation of clouds (Auligné et al 2010). In this section, we propose a method to analyse the homogeneity of the scene both in the observation space and in the model space.

The AVHRR cluster

The Advanced Very High Resolution Radiometer (AVHRR) on MetOp is helpful to define the scene type (partially cloudy or overcast).
The AVHRR cluster provided by EUMETSAT in the IASI level1c files (Cayla 2001) proved to be a valuable tool. This product is based on a radiance analysis of co-located AVHRR pixels inside each IASI FOV. AVHRR measures the radiance emitted by the Earth in six spectral bands: two in the visible and four in the IR.
All AVHRR pixels are aggregated in classes characterized by homogeneous properties in the radiance space using a K-means clustering. For each AVHRR class and each channel, the cluster product provides the mean radiance, the standard deviation and the coverage of the

class within the IASI pixel. As the aggregation was performed with all the available AVHRR channels, the algorithm can produce several classes even with relatively small standard deviations for the IR channel. As a result, a FOV with several classes with each one a small standard deviation and a mean radiance close to that of the other classes can be more homogeneous than a FOV with a single class. This is the reason why the number of AVHRR classes inside each IASI pixel was not used as the homogeneity criterion. Alternatively, these characteristics were used to compute global statistics of the AVHRR cluster aggregating the information provided by all the classes within the IASI FOV. We focused on one of the IR channels (11.5 μm) to get closer to the scene observed by IASI.

We calculated a weighted average considering each mean radiance and standard deviation for the 11.5 μm band (weight depending on the coverage of the class within the IASI pixel). One part of the homogeneity criterion is based on the relative standard deviation calculated from these global statistics and represents the intra-class homogeneity of the AVHRR cluster. This first criterion assures that each AVHRR class is homogeneous but not that all the classes observe the same cloudy scenes. To evaluate the inter-class homogeneity, the standard deviation of the mean radiances of all the classes has been calculated.

The AVHRR cluster gives information about the scene observed by IASI but none about AROME. To keep scenes for which both the observation and the simulated radiance are homogeneous, the model homogeneity has been evaluated by a comparable method.

Similar statistics as the ones used from the AVHRR cluster are reproduced. We used each AROME grid point within the IASI spot to simulate the radiances measured in the 11.5 μm band by the AVHRR imager with the use of the radiative transfer model RTTOVCLD. The standard deviation between each simulated radiance is the equivalent in the model space of the inter-class homogeneity and can be used to evaluate the model homogeneity (for more details on the process of selection see Martinet et al 2012(a)).

The concepts of inter-class and intra-class homogeneity in the model space and the observation space were used to select homogeneously covered cloudy scenes.

Evaluation of the observation operator

In this section, we monitor simulated and observed cloudy IASI radiances during our 30-day test period over the Mediterranean Sea.

To be assured that the monitoring focused on overcast scenes, the percentage of cloudy AVHRR pixels within the IASI FOV has been used in addition to the selection of homogeneous scenes. IASI observations with 100% of cloudy AVHRR pixels were kept.

In this screening-procedure, we imposed the cloudiness of the observation by the amount of cloudy AVHRR pixels within the IASI FOV but we did not take into account the cloudiness of AROME. To sidestep this problem and check that both the observation and the model observe the same cloudy scene, we imposed that the difference between the mean AVHRR brightness temperatures from the observed and the simulated cluster is smaller than 7K. This new constraint is important to avoid a cloud mislocation between AROME and IASI and to be as close as possible to the true state.

Standard deviations and biases of the O-B (observation minus background) departures are shown in figure 1 for the different screenings: overcast scenes (left panel), homogeneous overcast scenes (middle panel) and homogeneous overcast scenes with a condition on the AROME cloudiness (right panel). As should be expected, the best model statistics are found in channels least affected by clouds (CO2 and water vapour bands). Standard deviations are larger for window channels revealing a dependence on the vertical position of the sensitivity functions. Biases and standard deviations are large for overcast scenes (-7K and 20K respectively for window channels). The restriction to homogeneous scenes in both the model space and the observation space decreases the bias by 1K and the standard deviation by 4K in the window region. Thus, this criterion seems relevant to avoid the selection of broken clouds but it is not sufficient to have an acceptable level of bias prior to any assimilation. Avoiding

the cloud mislocation between AROME and IASI significantly improves the bias (-1K for window channels). The standard deviation is also decreased by more than 10K to values less than 5K which is a considerable improvement.

It is also interesting to investigate the PDF (probability density function) of the observation-operator error as it gives information on the observation-error covariance matrix **R**. For this study three channels spectrally located around 14 μm (700 cm-1, CO2 band, weighting function peaks around 250 hPa), 11 μm (942 cm-1, window channel, weighting function peaks around 1000 hPa) and 7 μm (1400 cm-1, water vapour channel, weighting function peaks around 500 hPa) were used. The PDF of the O-B departures are shown in figure 2, top panels for overcast scenes, middle panels for homogeneous overcast scenes and bottom panels for homogeneous overcast scenes with a condition on the AROME cloudiness (constraint on the AVHRR brightness temperature difference). The departures are characterized by a near-symmetric distribution for all channels. The skewness of the distribution is relatively small for CO2 and water vapour channels.

The impact of clouds is obvious on the window channel with departures spreading from -70K to 60K when considering only overcast observations. We can note that adding a constraint on the AROME cloudiness (bottom panels) narrower Gaussian distributions are observed for all channels with a significant improvement for the window channel. The departures for the window channel are significantly decreased spreading from -10K to 10K instead of -70K to 60K.

These results prove some capability of the observation operator to simulate overcast scenes. However, bias and standard deviation of the background brightness temperature compared with observations are large for channels highly sensitive to clouds. These channels are located in the window region and present large non-linearities in cloudy conditions. Without any bias correction, a screening only on the percentage of cloudy AVHRR pixels within the IASI FOV is not sufficient to assimilate these observations. The selection of homogeneous scenes with a constraint on the mean AVHRR brightness temperature enables to decrease the bias to a value more acceptable for the assimilation.

All these results support the idea that we should begin the assimilation by selecting observations of overcast clouds where an homogeneous FOV has been identified and where the NWP model is able to reproduce the observation homogeneity and cloudiness.

The selected homogeneous overcast clouds will be used in a 1D-Var retrieval process in the next section.

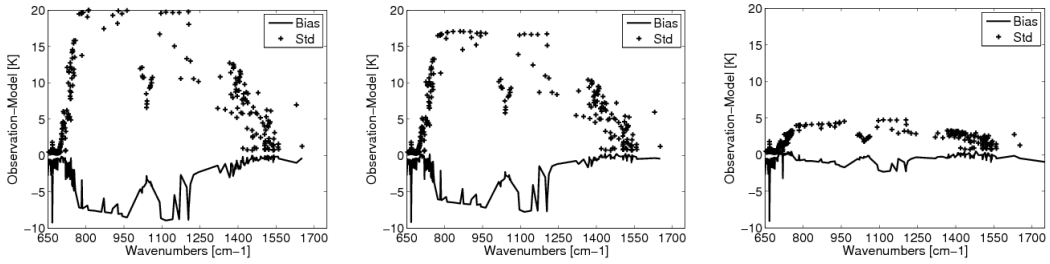

Fig 1: Bias and standard deviation (Std) of the differences between the model and the cloud-affected observed IASI brightness temperatures over a 30 day period from 7 October 2010 to 7 November 2010 on the Mediterranean Sea. Left panel: considering all overcast observations, middle panel: all homogeneous overcast scenes and right panel: only homogeneous overcast scenes with a constraint on the AVHRR brightness temperature.

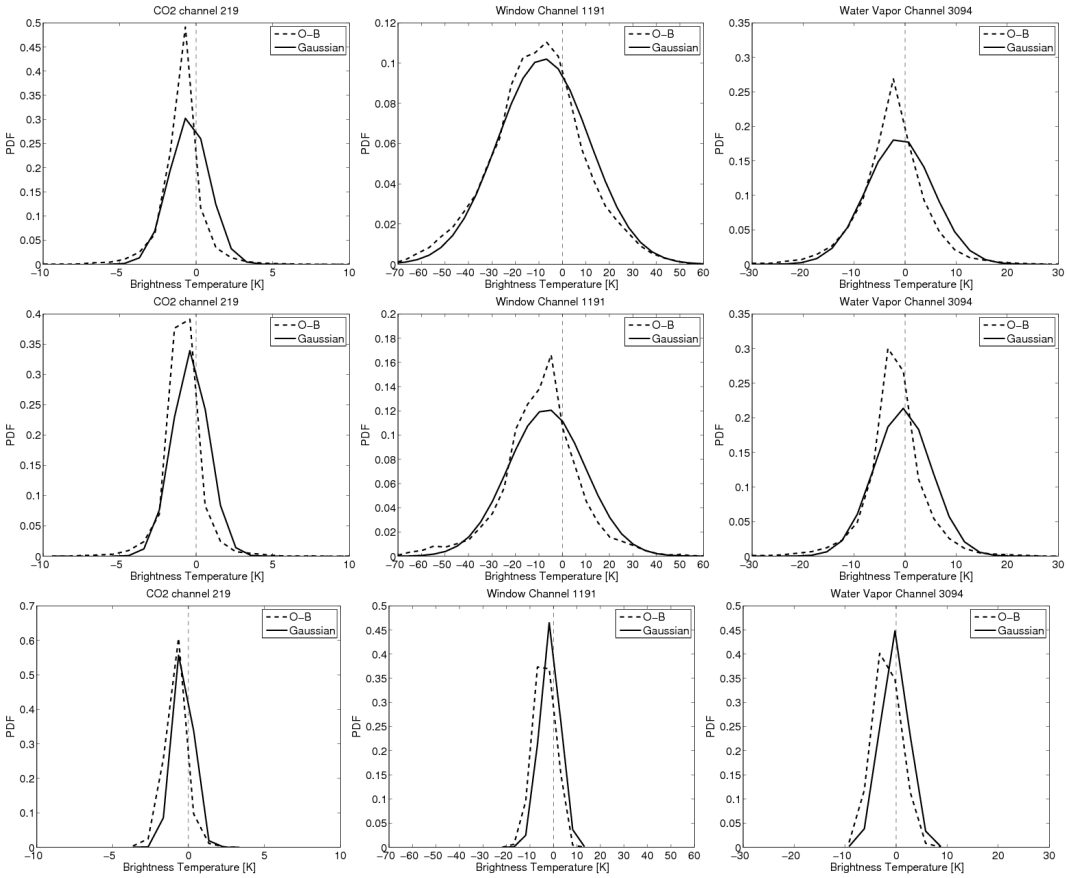

Fig 2: Relative frequency distribution of brightness temperature difference between observation and background (O-B) for all overcast scenes (top panel), homogeneously covered scenes (middle panels) and homogeneous scenes with a constraint on the AVHRR brightness temperature difference (bottom panels). The PDF are presented for three channels: (CO2 channel (14µm), window channel (12µm), water vapour channel (7µm)). The Gaussian distributions with the same error characteristics are also shown.

Observing System Simulation Experiments (OSSE) in a 1D-Var framework

In this section, 1D-Var experiments are performed using the 1D-Var code (version 3.3) provided by the Met Office in the frame of the EUMETSAT NWP Satellite Application Facility (Pavelin and Collard 2009). We interfaced this 1D-Var system with the version 10 of the RT model RTTOV and the cloud variables were added to the state vector.

As no observation is available to validate the retrievals, the 1D-Var is evaluated in the context of OSSE. For that purpose, the background profiles are generated from the AROME profile dataset perturbed with the addition of simulated forecast errors. The forecast errors are calculated from the error-covariance matrix **B**

such as :

$$\mathbf{x_b}=\mathbf{x_t}+\boldsymbol{\varepsilon_b}\mathbf{B}^{1/2}$$

where $\mathbf{x_b}$ is the perturbed background profile, $\mathbf{x_t}$ is considered as the `true' profile, and $\boldsymbol{\varepsilon_b}$ is a random number drawn from a Gaussian distribution with zero mean and unit standard deviation. The background-error statistics were derived from an AROME ensemble assimilation, that considers explicit observation perturbations and implicit background perturbations through the cycling, coupled with the operational ensemble assimilation at global scale. They were calculated from a set of 18 convective cases observed during the months of July, August and September 2009 (similar method detailed in Michel et al 2011).
The observations are generated from the perturbed background profiles and simulated observation errors are added such that:

$$\mathbf{y} = \mathbf{H}(\mathbf{x_t}) + \boldsymbol{\varepsilon_o}\mathbf{R}^{1/2}$$

where $\mathbf{y}$ is the perturbed observation, $\mathbf{H}(\mathbf{x_t})$ is the observation simulated from the `true' profile, and $\boldsymbol{\varepsilon_o}$ is a random number drawn from a Gaussian distribution with zero mean and unit standard deviation. The observation-error covariance matrix $\mathbf{R}$ was constructed with the values of the instrumental noise provided by CNES and a constant error is added to take into account the radiative transfer model error. In the context of cloudy retrievals, 200 channels have been added to the operational IASI selection of 366 channels used at ECMWF (Collard 2007, Collard and McNally 2009). The 200 channels have been chosen with the iterative method of Rodgers (2000) on profiles over the Mediterranean Sea homogeneously covered by clouds and representative of different cloud-types (semi-transparent ice clouds, opaque ice clouds, low liquid clouds, mixed-phase clouds).
The root-mean-square errors (RMSE) of the background and retrieved profiles with respect to the `truth' (i.e. the original AROME model profiles) are shown for high opaque clouds (figure 3) and low clouds (figure 4). The profiles of RMSE indicate that the analyses are always better than the background. Information about temperature, humidity, liquid water content and ice water content can be successfully extracted from the IASI cloudy soundings. In the opaque-cloud cases, the analysis errors are smaller than the background errors essentially for ice water content. The improvement for temperature is located above 200hPa because of the cloud opacity. For humidity and liquid water content, the background RMSE is almost equal to the analysis RMSE (not shown). In the low-cloud cases, the cloudy soundings contribute to temperature and humidity information through the entire atmospheric column. The 1D-Var also modifies liquid water content and ice water content profiles so as to fit better the `true' profiles.
To conclude, it appears that the assimilation of low-level and high-level opaque clouds may bring significant benefits for the extraction of cloud information. The information gained by opaque clouds is small for temperature and humidity however, but the information brought to ice water content is really encouraging.

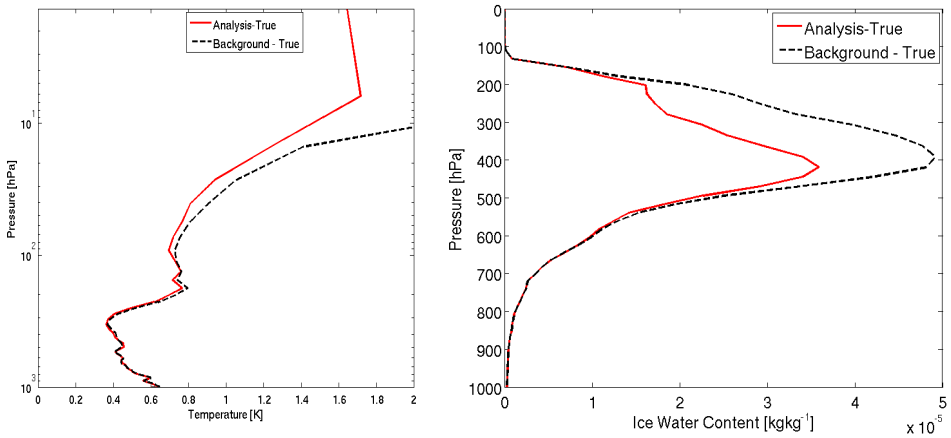

Fig 3: Root mean square errors between the background and the `true' profile (dotted line) and between the analysis and the `true' profile (thick red line). Retrievals considering high opaque clouds.

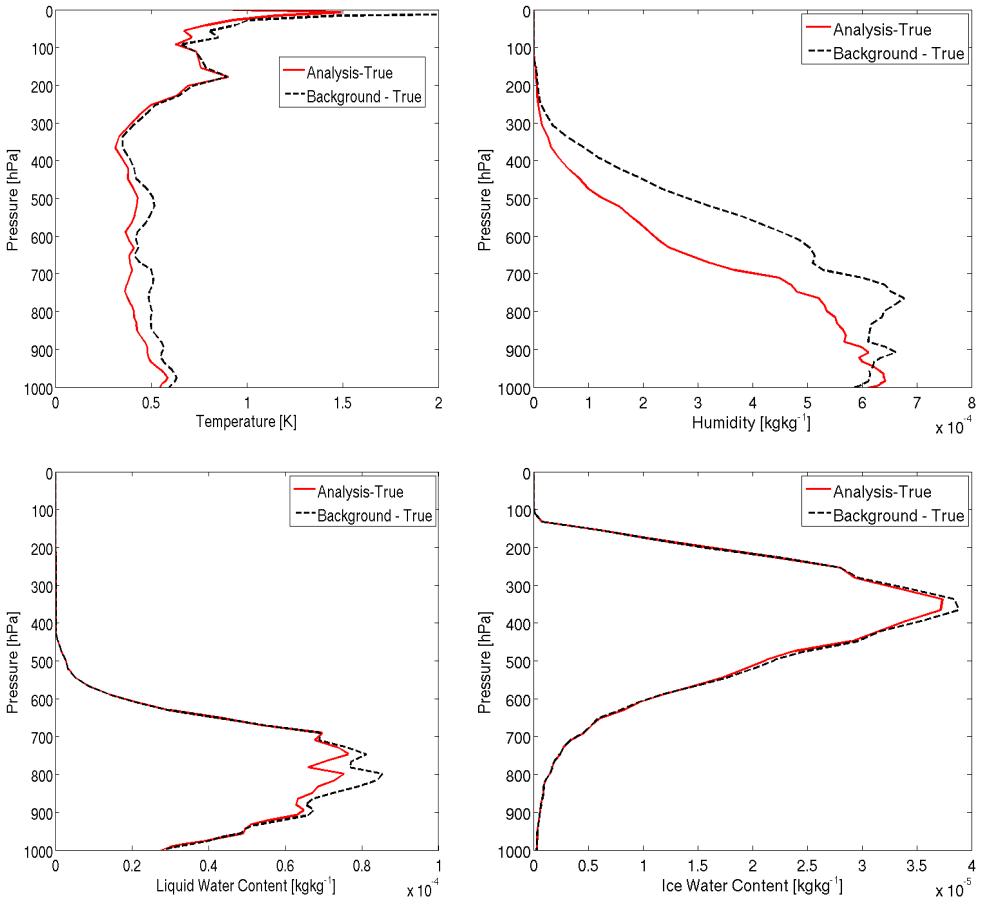

Fig 4: Root mean square errors between the background and the `true' profile (dotted line) and between the analysis and the `true' profile (red thick line). Retrievals considering low clouds.

Conclusion

In this paper, we evaluated the capability of using the cloud variables (liquid water content and ice water content) for the assimilation of cloud affected infrared radiances in convective scale models. The assimilation of radiances in such models suffers from sources of mismatch between the cloudy observations (IASI) and synthetic values simulated from clouds generated by AROME: bad location of clouds, representativeness, radiative transfer.

Before any assimilation, it is important to evaluate the observation operator used to calculate the background equivalents on a given selection of observations while minimizing all the sources of mismatch.

The first part of this paper presents an observation screening procedure to select cloudy scenes valuable for the assimilation. The radiance analysis of co-located AVHRR imager inside each IASI field of view has proved to be useful to quantify the degree of homogeneity of the scene. An equivalent of the AVHRR observations was simulated using the cloud profiles of each AROME grid point within the IASI field of view. A process based on the AVHRR cluster has been implemented to divide the observations between homogeneous and heterogeneous scenes. A significant improvement of the agreement between cloudy observations and simulations from AROME was observed.

The advanced interface RTTOVCLD was evaluated using our selection of homogeneous scenes. Biases of observation minus simulation differences were mainly negative showing an underestimation of the cloud radiative forcing. Large errors, both in terms of bias and standard deviation were shown for the most cloud affected channels. To avoid the model cloud mislocation, the cloudiness has been checked in both the model space and the observation space. This restriction enabled to significantly decrease biases and standard deviations.

The second part of the paper described some 1D-Var experiments. The retrievals were validated with OSSE. The root-mean-square-error of the retrieved profiles with respect to the `truth' is always better than the root-mean-square-error of the background with respect to the `truth'. An improvement of temperature and ice water content above the cloud top for opaque clouds was observed. Information on temperature, humidity, liquid water content and ice water content can be extracted through the entire column for low clouds.

This paper described a feasibility study to investigate the potential of cloud estimation to improve the use of cloud-affected radiances. Encouraging results have been found for the extraction of microphysical information. However, this study is restricted to the linear estimation theory for which the observation operator should be perfect and linear.

In cloudy conditions, the linearity of the observation operator is not respected but efforts have been made to select homogeneous cloudy scenes with small background departures to be already close to the `true' state. It has been shown that the observation selection was good enough to have an acceptable level of non-linearity in the observation operator. It was noted that opaque clouds were the most appropriate to respect the tangent-linear assumption.

In future, the potential benefit of using a flow-dependent **B** matrix representative of different cloud types should be investigated. For this study, the operational IASI channel selection has been reviewed to add new channels sensitive to cloud information (Martinet et al 2012(b)). This channel selection will be improved and evaluated on different air-mass types (polar, mid-latitude, tropical).

This work has been partly sponsored by MISTRALS/HYMeX programme.

References

- Auligné T, Lorenc A, Michel Y, Montmerle T, Jones A, Hu M, Dudhia J, 2010. Summary of the first International Cloud Analysis Workshops. *Bull.Amer.Meteor.Soc*., doi:10.1175/2010BAMS2978.1.
- Cayla F-R, 2001. AVHRR Radiance Analysis inside IASI FOV's. IA-TN-0000-2092-CNE, *CNES internal report.*
- Collard A, 2007. Selection of IASI channels for use in numerical weather prediction. *Quart.J.Roy.Meteor.Soc*., **133**, 1977-1991.
- Collard A,McNally A.P, 2009. The assimilation of Infrared Atmospheric Sounding Interferometer radiances at ECMWF. *Quart.J.Roy.Meteor.Soc*., **135**, 1044-1058.
- English S, Eyre J, Smith J, 1999. A cloud-detection scheme for use with satellite souding radiances in the context of data assimilation for numerical weather prediction. *Quart.J.Roy.Meteor.Soc*, **125**, 2359-2378.
- Fourrié N, Rabier F, 2004. Cloud characteristics and channel selection for IASI radiances in meteorologically sensitive areas. *Quart.J.Roy.Meteor.Soc*, **128**, 2551-2556.
- Hocking J, Rayer P, Saunders R, Matricardi M, Geer A, Brunel P, 2010. RTTOV v10 Users Guide.NWPSAF-MO-UD-023, EUMETSAT, Darmstadt, Germany.
- Kelly G, Thépaut J-N, 2007. Evaluation of the impact of the space component of the Global Observing System through Observing System Experiments. *In Proceedings of Seminar on recent developments in the use of satellite observations in numerical weather prediction*, ECMWF: Reading, UK. pp 327-348.
- Martinet P, Fourrié N, Guidard V, Rabier F, Montmerle T and Brunel P, 2012(a). Towards the use of microphysical variables for the assimilation of cloud-affected infrared radiances. *Quart.J.Roy.Meteor.Soc*, submitted.
- Martinet P, Lavanant L, Fourrié N, Rabier F, Faijan F, 2012(b). IASI channel selection in cloudy conditions. *In Proceedings of ITSC-18*, Toulouse, France, 21-27 March 2012.
- McNally A.P, 2002. A note on the occurrence of cloud in meteorologically sensitive areas and the implications for advanced infrared sounders. *Quart.J.Roy.Meteor.Soc* ,**128**, 2551-2556.
- McNally A.P and Watts P.D, 2003. A cloud detection algorithm for high spectral resolution infrared sounders. *Quart.J.Roy.Meteor.Soc*, **129**, 3411-3423.
- Michel Y, Auligné T, Montmerle T, 2011. Heterogeneous Convective-Scale Background Error Covariances with the Inclusion of Hydrometeor Variables. *Monthly Weather Review*, **139**, 2994-3015.
- Pavelin E.G, English S.J, Eyre J.R, 2008. The assimilation of cloud-affected infrared satellite radiances for numerical weather prediction. *Quart.J.Roy.Meteor.Soc*, **134**, 737-749.
- Pavelin E.G, Collard A, 2009. NWP SAF Met Office 1D-Var User Manual. NWPSAF-MO-UD-006.
- Rodgers CD, 2000. Inverse methods for atmospheric soundings: theory and practice. World Scientific: Singapore.
- Seity Y, Brousseau P, Malardel S, Hello G, Benard P, Bouttier F, Lac C, Masson V, 2011. The AROME-France convective-scale operational model. *Monthly Weather Review*, **139**, 976-991.